RZ 3543 (# 99555) 04/12/04
Mathematics & Physics 8 pages

Research Report

Characterization of Parallel Optical-interconnect Waveguides Integrated on a Printed Circuit Board

G.L. Bona,[1] B.J. Offrein,[1] U. Bapst,[1] C. Berger,[1] R. Beyeler,[1] R. Budd,[2] R. Dangel,[1] L. Dellmann,[1,3] and F. Horst[1]

[1]IBM Research GmbH
Zurich Research Laboratory
8803 Rüschlikon
Switzerland

[2] IBM Research
T.J. Watson Research Center
Yorktown Heights, NY 10598
USA

[3]Laboratory for Electromagnetic Fields and Microwave Electronics
Swiss Federal Institute of Technology, ETH-Zurich
Gloriastrasse 35
8092 Zurich, Switzerland

Characterization of parallel optical-interconnect waveguides integrated on a printed circuit board

G.L. Bona[*a], B.J. Offrein[a], U. Bapst[a], C. Berger[a], R. Beyeler[a], R. Budd[b], R. Dangel[a], L. Dellmann[a,c] and F. Horst[a]

[a] IBM Research GmbH, Zurich Research Laboratory, 8803 Rüschlikon, Switzerland;
[b] IBM Research, T.J. Watson Research Center, Yorktown Heights, NY 10598, U.S.A.;
[c] Laboratory for Electromagnetic Fields and Microwave Electronics, Swiss Federal Institute of Technology, ETH-Zurich, Gloriastrasse 35, 8092 Zurich, Switzerland

ABSTRACT

The development of optical interconnects in printed circuit boards (PCBs) is driven by the increasing bandwidth requirements in servers, supercomputers and switch routers. At higher data rates, electrical connections exhibit an increase in crosstalk and attenuation; which limits channel density and leads to high power dissipation. Optical interconnects may overcome these drawbacks, although open questions still need to be resolved. We have realized multimode acrylate-polymer-based waveguides on PCBs that have propagation losses below 0.04 dB/cm at a wavelength of 850 nm and 0.12 dB/cm at 980 nm. Transmission measurements at a data rate of 12.5 Gb/s over a 1-m-long waveguide show good eye openings, independent of the incoupling conditions. In the interconnect system, the transmitter and receiver arrays are flip-chip-positioned on the top of the board with turning mirrors to redirect the light. The coupling concept is based on the collimated-beam approach with microlenses in front of the waveguides and the optoelectronic components. As we aim for large two-dimensional waveguide arrays, optical crosstalk is an important parameter to be understood. Accordingly, we have measured optical crosstalk for a linear array of 12 optical channels at a pitch of 250 μm. The influence of misalignment at the transmitter and the receiver side on optical crosstalk will be presented as a function of the distance between waveguide and transmitter/receiver.

Keywords: polymer, multimode, optical waveguide, crosstalk, BERT, PCB, microlenses

1. INTRODUCTION

Servers, supercomputers and switch routers typically consist of multiple racks, where each rack has a backplane or midplane, and multiple plug-in cards (or blades). The increasing aggregate bandwidth, of the communication between the plug-in-cards that is routed through the backplane, drives the development of optical interconnects [1]. In order to make this transition to optical interconnects a reality, we need to integrate optical waveguide layers into the plug-in cards as well as into the backplane. The electro-optical elements, vertical surface-emitting lasers (VCSELs) and detectors, must be coupled to the optical waveguides, and there is a need for an optical card-to-backplane connector. In this paper we address the polymer optical waveguide technology in Section 2, present optical coupling experiments in Section 3 and describe system results of an on-board optical interconnect demonstrator in Section 4.

2. POLYMER WAVEGUIDE TECHNOLOGY

Polymer materials are generally recognized to exhibit various favorable properties for the use in optical waveguide technology [2]. There is a great potential for the use of polymers in terms of optical properties, cost-effectiveness, and processing possibilities. Different classes of eligible polymers are acrylates, siloxanes, polyimides, polycarbonates, and olefins [2]. With regard to optical backplane applications polymers have to fulfill tight requirements, such as very low optical losses and the compatibility with PCB manufacturing processes (e.g. resilience against solder reflow and lamination process). The optical propagation distance we anticipate is in the range of 30 to 100 cm and therefore the propagation losses should be below 0.05 dB/cm.

Allowing for these low losses and the required compatibility with PCB manufacturing, we evaluated different photosensitive polymer materials that are mainly based on acrylates.
The deposition of the liquid polymeric layers as claddings and waveguide cores on conventional FR4 substrates was done by doctor blading as well as by spray coating. The patterning of the core layer was performed photo-lithographically by UV exposure through a mask in proximity and by subsequent solvent developing. Thus, it was possible to realize arrays of multimode waveguides of 50 × 50 μm^2 cross-sectional area with 250 μm pitch as well as higher-density arrays of 35 × 35 μm^2 waveguides with 100 μm pitch (Figs. 1 and 2).

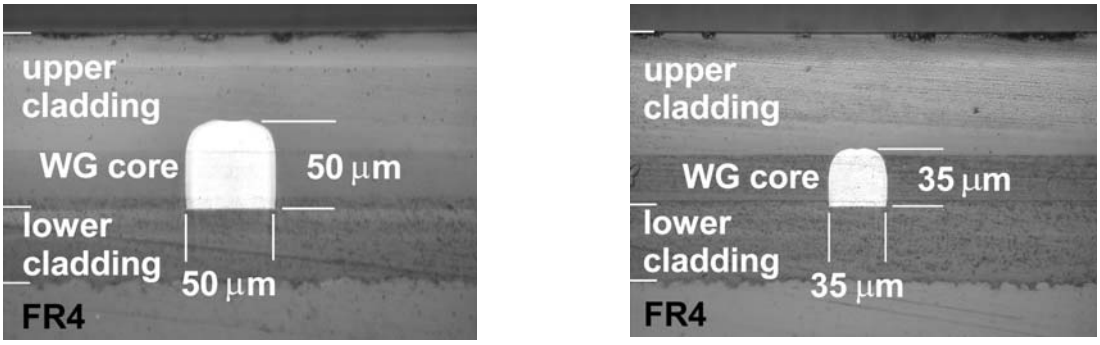

Figure 1. Cross-sections of 50 × 50 μm^2 and 35 × 35 μm^2 polymer waveguides on FR4 substrates.

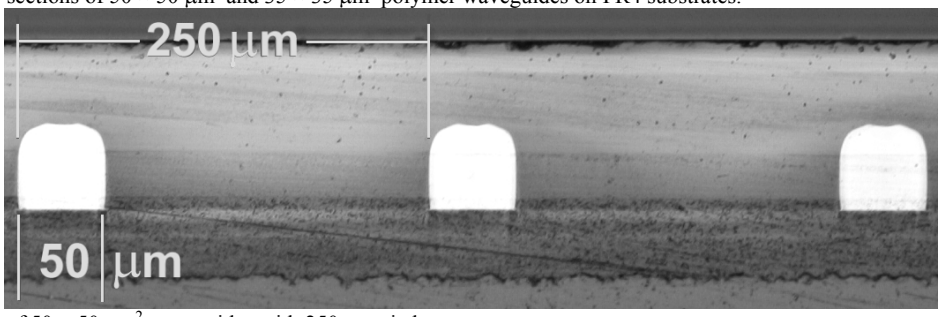

Figure 2. Array of 50 × 50 μm^2 waveguides with 250 μm pitch.

Initial fabrication issues such as dewetting, layer thickness inhomogeneities, material shrinkage, edge bead and polymerization inhibition by oxygen were resolved by process optimization.
In order to measure the waveguide propagation losses more accurately than the common cut-back method allows, we designed and fabricated a spiral-like waveguide path having a length of 100 cm on a board of 75 × 75 mm^2 area (Fig. 3). The loss values were determined by measuring the optical transmission of this waveguiding spiral in comparison with the transmission of 8.26-cm-long reference waveguides on the same board.

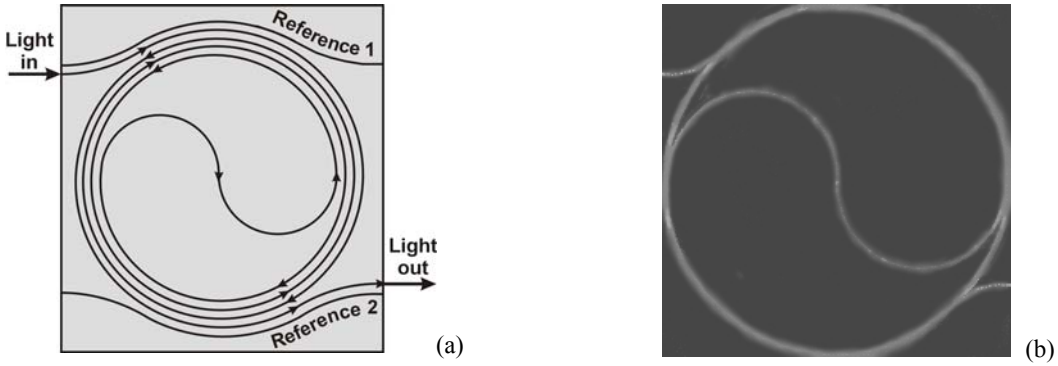

Figure 3. (a) Schematic of 100-cm-long waveguide spiral designed for loss and mode dispersion measurements.
(b) Top view of spiral illuminated by incoupled visible light of λ = 670 nm wavelength.

For some commercially available acrylate-based polymers we found very low waveguide propagation losses of 0.035 to 0.050 dB/cm at a wavelength of 850 nm. The waveguides having widths of 30 µm, 50 µm, and 70 µm showed consistent loss values, reflecting the smoothness of the waveguide sidewalls.
With regard to waveguide routing we also fabricated and characterized 90° waveguide crossings and y-splitters (Figs. 4a and 5a). We found an extremely low loss of 0.02 dB per crossing and almost perfect 1:1 splitting ratio with an excess loss of only 0.1 dB for $\lambda = 850$ nm (Figs. 4b and 5b).

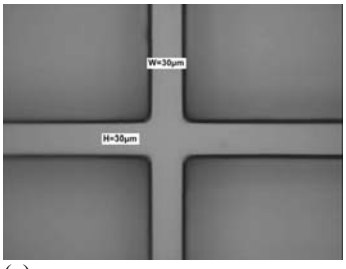

(a)

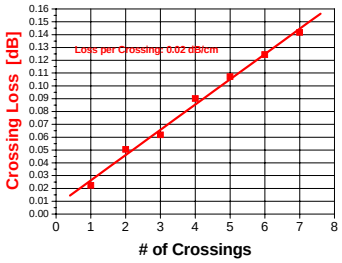

(b)

Figure 4. (a) Top view of 30-µm waveguide crossing. (b) Graph of measured loss depending on the number of crossings.

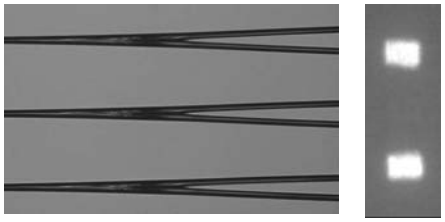

(a) (b)

Figure 5. (a) Top view of three 50-µm waveguide y-splitters. (b) Light detected at splitter output.

3. OPTICAL COUPLING

In incorporating optics into the PCB, we face various challenges. Besides the realization of the optical waveguides in or on the PCB, also the coupling between the electrical and the optical domain entails some specific issues. VCSELs and optical detectors that perform the required electro-optical and opto-electrical conversion are commercially available. The way they are integrated into the system is still open however and several arrangements have been proposed [3,4]. Two basic layout options are shown in Fig. 6. Either the opto-electronic components are positioned on top of the board or vertically in the board. In the latter layout, the optical system will be simpler but new packaging concepts are required to integrate the element vertically. In both options, a 90° bend has to be overcome: in the first option this is solved in the optical domain by a mirror and in the second option in the electrical domain by a flex cable.

(a) (b)

Figure 6. Schematic view of coupling concepts in which the opto-electronics is positioned (a) on top of the board or (b) in the board.

In this paper we focus on the first layout option and use a collimated-beam approach to bridge the distance between the transmitter/receiver and the waveguide. Therefore, lenses are attached in front of the opto-electronic elements and the waveguides such that the latter are located in the focal points of the corresponding lenses. The collimated beam approach is of special of interest as it relaxes the lateral alignment tolerances of the two lensed systems with respect to each other. Nevertheless, the positioning of the lenses with respect to the opto-electronic elements and the waveguides needs to be performed with a high precision of about ±5 µm. We are particularly interested in the limits of this approach, i.e. the maximum separation, the alignment tolerances and the optical loss and crosstalk values that can be achieved. As future systems will consist of arrays of optical channels in which the number of channels may be large, i.e. 48 for a 4×12 array arrangement, optical crosstalk is a parameter that has to be considered carefully.
Characterization experiments were performed on a layout, in which the VCSEL and detector arrays are positioned vertically with respect to the waveguide sample as shown in Fig. 7. The VCSEL is driven so as to characterize the VCSEL-to-waveguide coupling behavior, i.e. the optical power is coupled into the waveguide and imaged onto a detector

(Fig. 7a). To test the waveguide-to-detector coupling tolerances, 850-nm light from an external laser is coupled into the waveguide and imaged onto the detector as shown in Fig. 7b.

(a) (b)

Figure 7. Experimental arrangement to characterize the optical coupling behavior.

The electro-optical package is mounted onto a XYZ stage that is scanned to measure the coupling profiles. Figure 8 shows the coupling profiles for coupling in to and out of the waveguides as a function of the lateral displacement of the opto-electronic elements. The measurements were repeated for various lens-to-lens separations of up to 10 mm. The waveguide microlenses have an NA of 0.3 and the lenses on the opto-electronic elements have an NA of 0.4. The lens radius is 235 µm. The polymer waveguides have a 50 × 50 µm^2 cross section and an NA of 0.3.

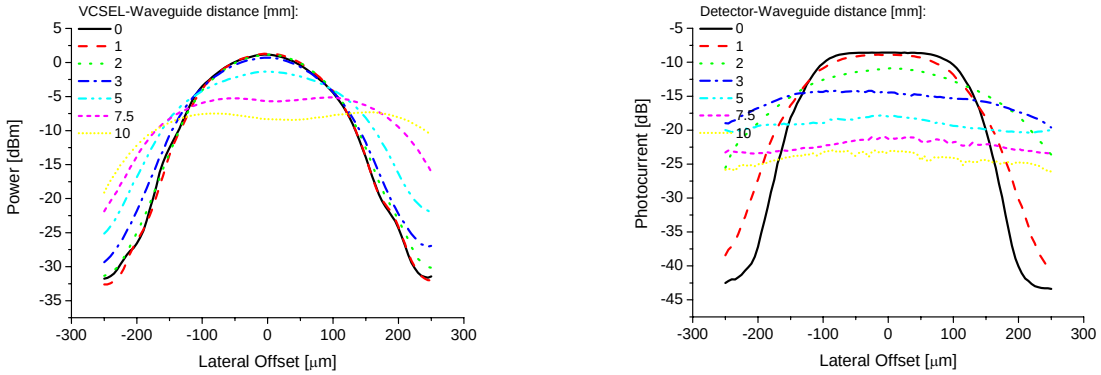

(a) (b)

Figure 8. Measured coupling profiles for coupling (a) in to and (b) out of the polymer waveguides.

To verify the validity of these experimental data, we also performed Monte-Carlo ray-trace simulations and found a good qualitative agreement as shown in Fig. 9.

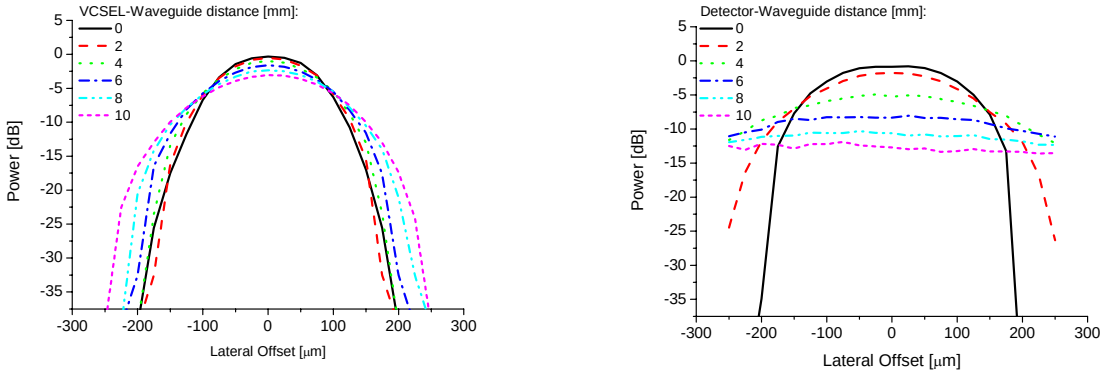

(a) (b)

Figure 9. Simulated coupling profiles for coupling (a) in to and (b) out of the polymer waveguides.

The optical crosstalk to the neighboring waveguides follows from the difference in optical power at zero lateral offset and at the *x*-axis positions at ±250 µm. For the in-coupling case, the optical power and the crosstalk exhibit a relatively large tolerance with respect to the lens-to-lens distance (Fig. 8a), whereas the out-coupling from the waveguide to the detector is much more sensitive to the distance (Fig. 8b). This is due to the difference in the apertures of the VCSEL and the waveguide. The VCSEL has a diameter of about 10 µm, which is small with respect to the waveguide pitch of 250 µm. Therefore a collimated beam is formed with a small divergence. The waveguide size of 50 µm causes a much larger divergence of the collimated beam, which introduces a critical sensitivity to the lens-to-lens separation.

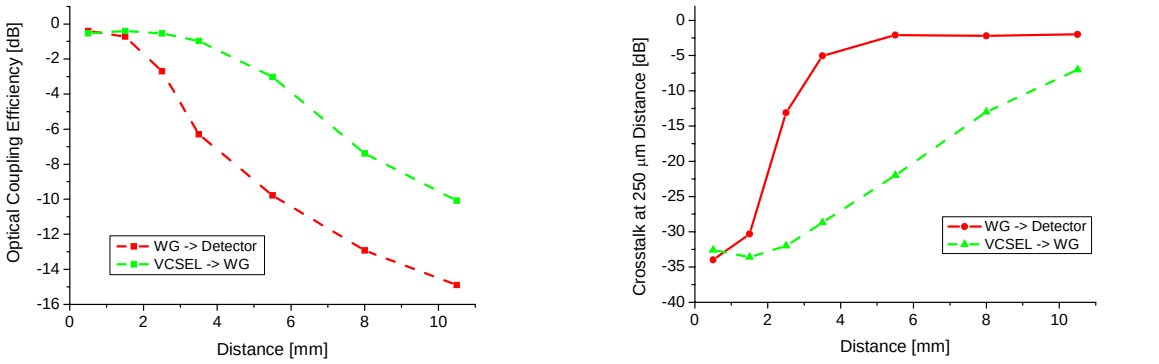

(a) (b)

Figure 10. (a) Optical coupling loss and (b) optical crosstalk as a function of the lens-to-lens separation.

The alignment of the lenses with respect to the opto-electronic elements and the waveguides needs to be performed with precision, i.e. with an accuracy of about ±5 µm. The alignment of the optical package containing the lensed opto-electronic components, with respect to the lensed waveguides is therefore much more relaxed, i.e. about ±50 µm for a 1 dB loss penalty. This is the main advantage of the collimated beam approach. Nevertheless, for a 1 dB loss penalty and a crosstalk level below -25 dB, the distance between the waveguides and the package that can be bridged is limited to 1.7 mm.

4. SYSTEM MEASUREMENTS

Figure 11 shows a schematic side view of our demonstrator setup that was designed to serve as a general test platform for various aspects of our multi-disciplinary effort. Arrays of 1×12 waveguides (A) with a core size of 50 µm and a pitch of 250 µm were fabricated on top of a commercially manufactured PCB (B). Pads (C) for connecting the opto-electronic packages (D) were placed on both sides of the board in order to be able to implement both the situation of waveguides on the surface and that of buried waveguides. So far, only the first situation has been experimentally tested because of the lens-to-lens distance limitations discussed in Section 3. By extending the waveguides to the board edges and by cutting the waveguide access slots (E) separately, we have the freedom to realize various configurations (different coupling modules, but also on-board vs. off-board links) with the same hardware. For the on-board link presented here, two slots (E) for the coupling optics (F&G) were cut into the board. The board-side part of the coupling optics, namely a microlens-array (F) collimating the waveguide output and a mirror (G) for the 90°-bend, were mounted in place separately. A 1×4 array of VCSELs (H) [5] and a 1×4 array of photodetectors [6] (both designed for 10 Gb/s operation at 850 nm) were mounted with a precision of ≤5 µm into the cavity (J) of a high-speed-capable surface laminate organic package using a chip-transfer method [7]. With the same method (but currently with less precision), the populated package was attached to an aluminum frame (K) with alignment pinholes and fixture threads. After wire bonding, an array of microlenses (L) was mounted on top of the opto-electronic chips to collimate/focus the emerging/incident light. The finished package was electrically contacted by means of a Fujipoly ZEBRA® W Series elastomeric connector (M) [8] and mechanically clamped to the board with two alignment pins and four screws (N). Because of space constraints and other boundary conditions, only 2×1 of the 2×4 available channels can be contacted with high-speed-capable SMA connectors (O).

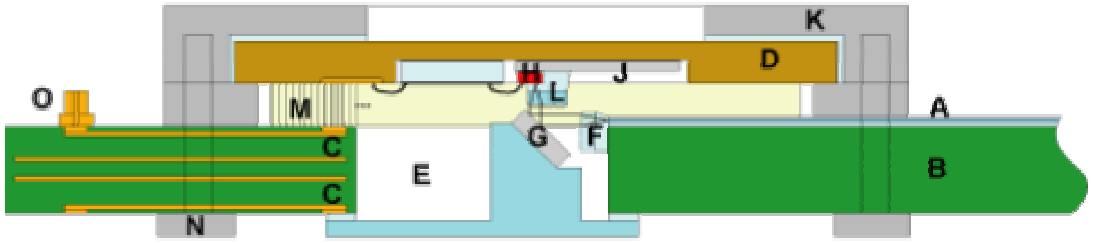

Figure 11. Side view of electro-optical package and coupling optics. See text for explanation.

Once all the individual building blocks were ready, they were assembled to a demo board (photo with top view shown in Fig. 12a) and connected to our high-speed test equipment (Fig. 12b). With this setup, we were able to demonstrate multiple Gb/s signal transmission from the Tx module to the Rx module. Figure 12c shows a 5 Gb/s eye diagram without any pre-conditioning of the modulation signal. In Fig. 12d we demonstrate a 10 Gb/s eye diagram, in which the higher frequencies of the VCSEL modulation signal have been slightly emphasized by applying a digital feed-forward response (FIR) filter.

(a)

(b)

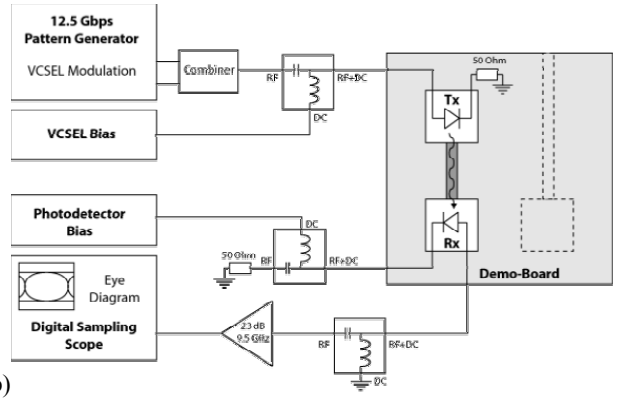

(c)

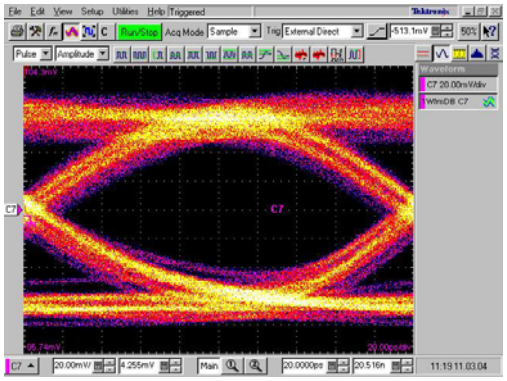

(d)

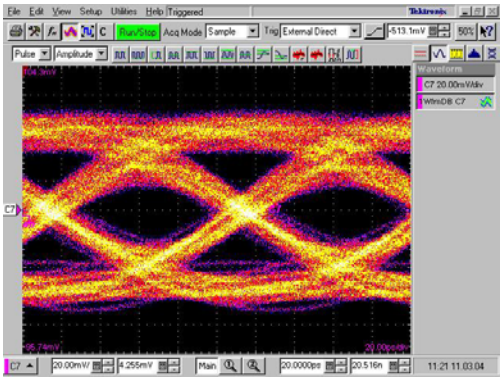

Figure 12. (a) Photo of populated demonstrator board. (b) Scheme of measurement setup. (c) Eye diagram at 5 Gb/s without any signal preconditioning. (d) Eye diagram at 10 Gb/s with some pre-emphasis on the higher frequencies using an FIR filter.

The overall speed is currently limited by the electrical path (multiple cascaded wire bonds and the ZEBRA® connector) and by the distance of approx. 60 cm between the photodetector and the currently external amplifier. Tests with the Tx-part alone (Fig. 13a) showed clean, open eyes at 12.5 Gb/s at the edge of the Tx-board (Fig. 13b).

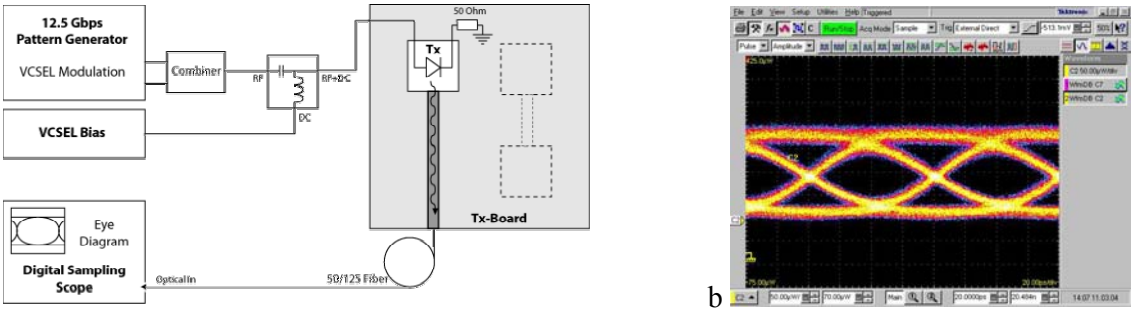

a b

Figure 13. a) Setup to test the Tx-part alone. (b) 12.5 Gb/s eye diagram, measured at the edge of the Tx board.

Measurements to extend the on-board link to a board-to-board link are currently underway. A first test in this direction was an experiment in which a 12.5 Gb/s signal (provided by a commercial 10 Gb/s VCSEL) was sent through a 1-m-long waveguide fabricated as a spiral on an FR4 substrate as described in Section 2. Figure 14a shows the setup and Fig. 14b the eye diagram measured at the output of the 1 m spiral. This result already confirms that at this length and datatrate modal dispersion will not be of particular concern.

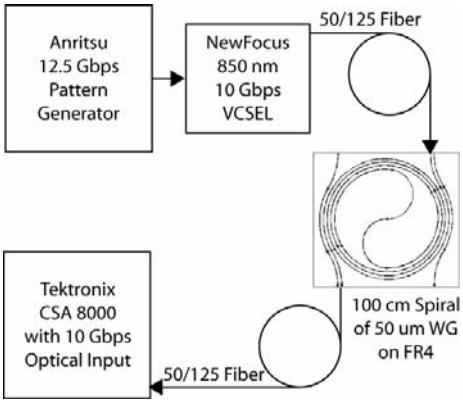

(a)

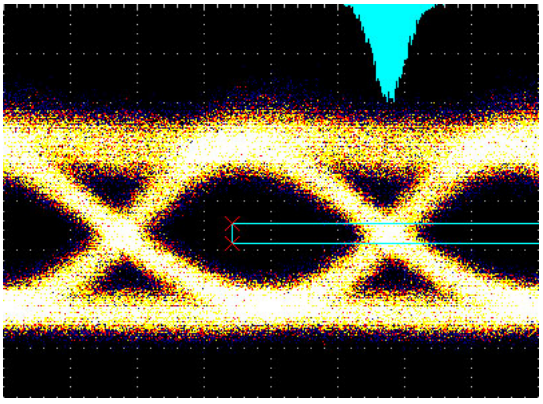

(b)

Figure 14. (a) Long waveguide measurement setup. (b) Eye diagram at 12.5 Gb/s after propagation through the 1 m waveguide spiral (50 μm core).

4. SUMMARY AND OUTLOOK

We have demonstrated an parallel optical interconnect demonstrator using low loss, multimode polymer waveguide arrays on a PCB. The opto-electronic components were mounted in a high-speed organic package and the optical coupling was solved efficiently by microlens arrays and 45° mirrors. System-level tests of our first demonstrator setup were successful up to 10 Gb/s. The limits in density, optical performance as well as coupling trade-offs were discussed. In the next steps we will study concepts with waveguides laminated into the board, as well as improve the coupling concepts to achieve cost-efficient, passively aligned positioning of the opto-electronic elements. These are prerequisites in order to have this kind of technology become reality in future products.

REFERENCES

1. D.A.B. Miller, “Rationale and Challenges for Optical Interconnects to Electronic Chips,” Proc. IEEE, **88**, pp. 728-749, 2000.
2. L. Eldada and L. W. Shacklette, "Advances in polymer integrated optics," *IEEE J. Select. Top. Quant. Electron.* **6**, 54, (2000).
3. E. Griese, “A High-Performance Hybrid Electrical-Optical Interconnection Technology for High-Speed Electronic Systems,” IEEE Trans. Advanced Packaging, **24**, pp 375-383, 2001.
4. Y. Ishii, N. Tanaka, T. Sakamoto, H. Takahara, “SMT-Compatible Large-Tolerance “OptoBump” Interface for Interchip Optical Interconnections,” IEEE Trans. Advanced Packaging, **26**, pp 122-127, 2003.
5. VCSELs by Avalon Photonics
6. Photodetectors by Albis Optoelectronics
7. X. Zheng, et al., "Optomechanical Design and Characterization of a Printed-Circuit-Board-Based Free-Space Optical Interconnect Package," *Appl. Opt.* **38** (26), 5631-5640, 1999.
8. http://www.fujipoly.com, ZEBRA® W Series Elastomeric Connectors.